Bcl-3 deficiency protects against DSS-induced colitis in the mouse

Christine O'Carroll[1], Gerard Moloney[1], Grainne Hurley[1], Silvia Melgar[1], Elizabeth Brint[1], Kenneth Nally[1], Robert J. Nibbs[2], Fergus Shanahan[1], Ruaidhrí J. Carmody*[2].

[1]Alimentary Pharmabiotic Centre, University College Cork, Ireland

[2]Centre for Immunobiology, Institute of Infection, Immunity and Inflammation, College of Medicine, Veterinary and Life Sciences, University of Glasgow, Glasgow, United Kingdom

Running title: Bcl-3 and colitis

***Corresponding author:** ruaidhri.carmody@glasgow.ac.uk

Disclosures: The authors have no conflict of interest to declare.

This article has been accepted for publication and undergone full peer review but has not been through the copyediting, typesetting, pagination and proofreading process, which may lead to differences between this version and the Version of Record. Please cite this article as doi: 10.1111/cei.12119

Summary

Bcl-3 is a member of the IκB family of proteins and is an essential negative regulator of Toll-like receptor induced responses. Recently, a single nucleotide polymorphism associated with reduced Bcl-3 gene expression has been identified as a potential risk factor for Crohn's disease. Here we report that in contrast to the predictions of SNP analysis, patients with Crohn's disease and ulcerative colitis demonstrate elevated Bcl-3 mRNA expression relative to healthy individuals. To further explore the potential role of Bcl-3 in inflammatory bowel disease (IBD) we used the dextran-sodium sulphate (DSS) induced model of colitis in Bcl-3$^{-/-}$ mice. We found that Bcl-3$^{-/-}$ mice were less sensitive to DSS-induced colitis compared to wild type controls and demonstrated no significant weight loss following treatment. Histological analysis revealed similar levels of oedema and leukocyte infiltration between DSS treated wild type and Bcl-3$^{-/-}$ mice but showed that Bcl-3$^{-/-}$ mice retained colonic tissue architecture which was absent in wild type mice following DSS treatment. Analysis of the expression of the pro-inflammatory cytokines IL-1β, TNFα and IL-6 revealed no significant differences between DSS-treated Bcl-3$^{-/-}$ and wild type mice. Analysis of intestinal epithelial cell proliferation revealed enhanced proliferation in Bcl-3$^{-/-}$ mice which correlated with preserved tissue architecture. Our results reveal that Bcl-3 has an important role in regulating intestinal epithelial cell proliferation and sensitivity to DSS induced colitis which is distinct from its role as a negative regulator of inflammation.

Introduction

The NF-κB transcription factor family controls the inducible expression of more than 500 genes, including cytokines, chemokines and regulators of cell survival and proliferation[1, 2]. The dual role of NF-κB as a key regulator of inflammation and cell survival makes it a critical factor in the pathogenesis of chronic diseases such as IBD. Increased NF-κB activation is observed in the mucosa of IBD patients and the requirement for NF-κB for the expression of pro-inflammatory cytokines supports a contributory role for NF-κB in IBD[3, 4]. Indeed, in the IL-$10^{-/-}$ mouse model of colitis, increased activation of NF-κB in myeloid cells is critical for the development of disease, while mice lacking CYLD or A20, two important negative regulators of NF-κB, show increased sensitivity to dextran-sodium sulphate (DSS)-induced colitis[4-7]. Moreover, the pharmacological inhibition of NF-κB by anti-sense oligonucleotides or inhibitory peptides can prevent DSS-induced colitis in mice[8].

Genetic studies have identified an equally important role for NF-κB in maintaining the homeostasis of the intestinal epithelium. Mice lacking NF-κB essential modulator (NEMO) in intestinal epithelial cells ($NEMO^{\Delta IEC}$) develop spontaneous and severe colitis resulting from elevated intestinal epithelial cell apoptosis[4, 9]. A similar phenotype is observed in mice lacking both the IKKα and IKKβ subunits in intestinal epithelial cells ($IKK\alpha\backslash\beta^{\Delta IEC}$) and mice lacking the NF-κB subunit RelA in intestinal epithelial cells are hypersensitive to DSS-induced colitis[4, 10]. Toll-like receptors (TLRs) are the key sensors of microbial products in innate immunity and appear to be critical in initiating NF-κB activation in intestinal epithelial cells. Thus, mice lacking MyD88, a key component downstream of a number of TLRs, are also hyper-responsive to DSS-induced colitis [11, 12]. Together these studies indicate that while NF-κB activity is critical for inflammation in IBD,

NF-κB activity in the epithelium is critical for tissue homeostasis and its inhibition can have severe consequences including the development of IBD. Thus a further understanding of the regulation of NF-κB during inflammation in the intestine and the contribution of components of the NF-κB pathway to inflammation and epithelial proliferation in the mucosa, are critical for the development of effective therapies for IBD.

Bcl-3 is a member of the IκB family of proteins as determined by sequence homology and the presence of ankyrin repeat domains which mediate interaction with NF-κB dimers [13-15]. Bcl-3 is largely a nuclear protein and only binds homodimers of the p50 or p52 NF-κB subunits[14]. Interestingly, these two subunits lack a transactivation domain and thus have generally been regarded as repressors of NF-κB transcription when present in the homodimeric form. Bcl-3 is an essential negative regulator of TLR induced responses. Bcl-3$^{-/-}$ macrophages and mice are hyper-responsive to TLR stimulation and are defective in lipopolysaccharide tolerance[16]. Recently, a single nucleotide polymorphism (SNP) associated with reduced Bcl-3 gene expression has been identified as a potential risk factor for Crohn's disease[17]. However, the role of Bcl-3 in IBD has not been investigated to date.

Here we report that our measurements of Bcl-3 mRNA in patient groups with Crohn's disease, ulcerative colitis and healthy individuals reveal elevated Bcl-3 expression associated with IBD, in contrast to the predictions of the SNP analysis[17]. To further explore the potential role of Bcl-3 in IBD we used the DSS-induced model of colitis in Bcl-3$^{-/-}$ mice. Considering the previously described anti-inflammatory role of Bcl-3 we were surprised to find that Bcl-3$^{-/-}$ mice were less sensitive to DSS-induced colitis. Measurement of the inflammatory response in the colon by analysis of the expression levels of pro-inflammatory cytokines and the recruitment of T-cells, neutrophils, macrophage and dendritic cells, revealed no significant differences between DSS-treated Bcl-3$^{-/-}$ and wild type mice. Analysis of intestinal epithelial cell death and proliferation revealed increased proliferation and

regeneration of the epithelium in Bcl-3$^{-/-}$ mice identifying Bcl-3 is an important factor in regulating epithelial cell turnover and sensitivity to colitis. Our study suggests that Bcl-3 may be an effective target for promoting regeneration of the epithelium in the colon.

Materials and Methods

Mice

Bcl3$^{-/-}$C57BL/6 (B6) mice were generated as described previously[15, 16]. All mice were group housed in individually ventilated cages (IVC's) under Specific Pathogen Free conditions. Standard housing and environmental conditions were maintained (temperature 21°C, 12 hours light & 12 hours darkness with 50% humidity). Animals were fed sterile standard pellet diet & water *ad libitum*. Animal husbandry and experimental procedures were approved by the University College Cork Animal Experimentation Ethics Committee (AEEC).

DSS induced Colitis

Mice were administered 2% dextran sodium sulphate (DSS) (45 kDa; TdB Consultancy) *ad libitum* in their drinking water to induce colitis as previously described[18]. DSS solutions were prepared freshly and administered on a daily basis for six days. This was followed by water up to day eight to induce acute disease. Body weight, stool consistency and posture/fur texture were recorded daily to determine the daily disease activity index (DAI). DAI scoring was assessed blinded with a maximum score of 10 as previously described[18, 19]. DAI scoring combined scoring from weight loss (% change) 0 – 4, stool consistency 0 – 4 and posture/fur texture 0 – 2. Briefly, a percentage weight loss score of 0 = no loss, 1 = 1 - 3% loss, 2 = 3 - 6% loss, 3 = 6 - 9% loss and 4 = greater than 9% loss in body mass. A stool consistency score of 0 = no change, 1 = mild change, 2 = loose stool, 3 = loose stool and rectal bleeding, 4 = diarrhoea and rectal bleeding. A fur and posture score 0 = no change, 1 = mild hunched posture, 2 = hunched posture and reduced movement. Mice were sacrificed at day 8 with colons removed from anus to caecum and washed in PBS. Colons were measured

and cut longitudinally dividing into the distal and proximal colon. Both proximal and distal colons were weighed and processed for histology, protein and qRT-PCR analysis.

Colon Histology

Distal colons (3cm) were cut longitudinally and into three sections. One section was rolled in a "swiss roll" fashion and frozen in OCT tissue freezing medium (Tissue-Tek) using liquid nitrogen. Frozen sections (6μm) were fixed in an ice cold acetone/ethanol 3:1 solution and stained with haematoxylin and eosin according to standard histological staining procedures. Stained sections were analysed and scored using a light microscope (Olympus BX51, Olympus, Germany). Images were captured using Cell F software (Olympus). Images captured are representative of greater than seven fields of view at 20X magnification per mouse. Histological scoring was performed in a blinded fashion. Scoring of tissue damage was quantified as previously described with a maximum combined score of 12 [19, 20] as follows: 0 – no infiltration, no injury, no crypt damage; 1- minor infiltration, mucosal injury, damage at crypt base; 2 – moderate infiltration (foci formation), mucosal and sub mucosal injury, damage at crypt base and centre; 3 – severe infiltration, transmural injury, only epithelium intact; 4 – loss of whole crypt and epithelium.

Gene expression analysis

Distal colon tissue gene expression was measured by quantitative real time PCR (qRT-PCR). Distal colons (3cm) were divided into three sections with one section frozen at -80°C in RNAlater (Sigma). Colon tissue samples were thawed on ice and transferred to magNALyser green bead tubes (Roche) and homogenised using the magNALyser homogeniser three times for 15 seconds at 6500 x g (Roche). Colonic tissue was homogenised in RLT lysis buffer (Qiagen) with homogenised samples centrifuged for 5 minutes at 4°C at 200 x g. Supernatants were stored at -80°C until required. Total RNA was

extracted using the RNeasy mini kit (Qiagen). 1µg total RNA was used to synthesise cDNA with random hexamer primers using Transcriptor Reverse Transcriptase (Roche). qRT-PCR was performed using the LightCycler 480 (Roche). Primers were designed using the Universal Probe Library system (Roche) as follows: IL-6 (Forward = tctaattcatatcttcaaccaagagg, Reverse = tggtccttagccactccttc); TNF-α (F = tcttctcattcctgcttgtgg, R = ggtctgggccatagaactga); IL-1β (F= tgtaatgaaagacggcacacc, R= tcttctttgggtattgcttgg); CXCL1 (F = agactccagccacactccaa, R= tgacagcgcagctcattg); IL-22 (F = tttcctgaccaaactcagca, R = ctggatgttctggtcgtcac); and IL-17A (F= cagggagagcttcatctgtgt, R= gctgagctttgagggatgat) was measured and normalised to 18S (F = aaatcagttatggttcctttggtc, R = gctctagaattaccacagttatccaa). Gene expression changes calculated using the 2-ΔΔCT method.

Human tissue arrays (Crohn's/Colitis cDNA Array, Origene) were used to measure Bcl-3 expression. Gene expression was measured using the LightCycler 480 system in combination with Taqman gene expression assay for Bcl-3 (Applied Biosystem). Relative mRNA was calculated using the 2-ΔΔCT method. Transcriptional profiling of Crohn's disease and Ulcerative colitis tissue was performed using a dataset of sigmoid biopsy patient samples published by *Costello et al*. (GEO dataset ID GDS1330) [21] (Crohn's disease n=10, Ulcerative Colitis n=10, normal controls n=11).

TUNEL

The extent of apoptosis in colonic tissue between groups was measured by terminal deoxynucleotidyl transferase-mediated deoxyuridine triphosphate nick end labelling (TUNEL). 6µm colonic tissue sections were incubated with 3% H_2O_2 and a 4% DEPC solution to eliminate background from both peroxidise and endonuclease enzyme activity in the tissue. The colon sections were incubated for one hour in a reaction using Terminal Deoxynucleotidyl Transferase (Promega) and Fluorescein 12- dUTP (Roche). Nuclei were

counterstained with Hoechst (Molecular Probes). Stained sections were analysed using a fluorescence microscope (Olympus BX51, Olympus, Germany). Fluorescence images were captured using Cell F software (Olympus). Images captured are representative of greater than seven fields of view at 20X magnification per mouse.

Immunofluorescence staining

Frozen sections (6μm) were fixed in an ice cold acetone/ethanol 3:1 solution and blocked with blocking buffer (10% serum, 5% fish gelatine, 0.05% Tween-20, 1% BSA, 0.1% sodium azide). Colon sections were incubated with anti-mouse Ki67 (Biolegend) and counterstained with Hoechst (Molecular Probes). Stained sections were mounted with Prolong Gold antifade mounting medium (Molecular probes) and visualised using a fluorescence microscope (Olympus BX51, Olympus, Germany). Fluorescence images were captured using Cell F software (Olympus). Images captured are representative of greater than seven fields of view at 20X magnification per mouse.

Western blotting

Frozen distal colon tissue samples were thawed, transferred to magNALyser green bead tubes (Roche) and homogenised using the magNALyser homogeniser three times for 15 seconds at 6500 x g (Roche). Total protein was isolated by lysing the distal colon tissue in RIPA buffer (150 mM NaCl, 50 mM Tris-Cl, pH 7.4, 1% NP-40, 0.25% sodium deoxycholate, 1mM Na_3VO_4, 1mM EDTA) supplemented with a protease and phosphatase inhibitor cocktail (Sigma). Total protein was resolved by SDS-PAGE gels, transferred to PVDF membrane and immune blotted for cleaved Caspase-3 (Cell signalling), and β-actin (Sigma).

Statistical analysis

Statistical analysis was determined using one-way ANOVA/ two-way ANOVA with post hoc analysis (Tukey's post hoc test and Bonferroni post hoc test). qRT-PCR expression data was calculated using the 2-ΔΔCT followed by unpaired *t* test and Mann Whitney *t* test to compare differences between groups. Statistical analysis was performed using GraphPad software (San Diego, CA, USA). Data is represented by mean +/- SEM with $p<0.05$ considered statistically significant.

Results

Elevated BCL3 mRNA is found in the colon of IBD patients

To assess the role of Bcl-3 in inflammatory bowel disease we initially analysed the Bcl-3 expression levels from a previously published study which identified a large number of genes associated with inflammatory bowel diseases[21]. In that study, transcriptional profiles were generated from biopsies taken from the sigmoid colon of patients with Crohn's disease (CD) (n=10) and Ulcerative Colitis (UC) (n=10) and those of normal controls (n=11). Our bioinformatics analysis of this dataset revealed that Bcl-3 mRNA expression levels were significantly increased in both CD ($p<0.01$) and UC ($p<0.05$) (Supplementary Figure 1). The elevated Bcl-3 mRNA levels in CD and UC were unexpected considering a SNP in the *BCL3* locus predicted to reduce expression of Bcl-3 mRNA was associated with in CD [17]. To confirm our analysis we next measured Bcl-3 mRNA expression by real time quantitative PCR (qRT-PCR) in an additional, independent patient cohort of 21 CD, 21 UC and 6 normal control colon tissue samples. Importantly, this independent analysis of Bcl-3 mRNA expression also revealed a statistically significant increase in Bcl-3 gene expression in Crohn's disease tissue samples relative to normal healthy controls ($p<0.05$) (Figure 1A). Moreover, the magnitude of increase of Bcl-3 mRNA levels in CD and UC relative to normal controls was similar in our tissue samples and in those contained in the previous microarray analysis. Next we measured Bcl-3 gene expression levels in WT mice receiving 6 days treatment with 2% dextran sodium sulphate (DSS) followed by 2 days without DSS to induce colitis. We found an increase in Bcl-3 mRNA in WT DSS treated mice relative to untreated control mice (Figure 1B). Taken together, these data demonstrate a strong correlation between increased Bcl-3 mRNA expression and colitis in both a murine model and human IBD.

Bcl-3$^{-/-}$ mice are protected against DSS-induced colitis

In order to further investigate the potential role of Bcl-3 in IBD we performed DSS-induced acute colitis in Bcl-3$^{-/-}$ and WT litter mate controls. WT and Bcl-3$^{-/-}$ mice were treated with 2% DSS in their drinking water for six days after which they were monitored for an additional two days, during which time they received normal drinking water. Within four days of beginning DSS treatment both Bcl-3$^{-/-}$ and WT mice developed characteristic symptoms associated with DSS-induced colitis. These included hunched posture and changes in stool consistency including rectal bleeding and diarrhoea. By day eight following DSS treatment WT mice had lost greater than 12% of their body weight (Day 6; $p<0.01$, Day 7; $p<0.001$, Day 8; $p<0.001$; Figure 2A). In contrast, DSS treated Bcl-3$^{-/-}$ mice did not demonstrate any significant loss of body mass when compared to untreated Bcl-3$^{-/-}$ mice up to 8 days following the initial DSS treatment (Figure 2A). When rectal bleeding, diarrhoea, hunched posture, and weight loss of DSS treated and untreated mice were scored and combined to give a daily activity index score (DAI) we found that Bcl-3$^{-/-}$ mice develop a significantly less severe form of DSS-induced colitis (Figure 2B). The reduced disease observed in Bcl-3$^{-/-}$ mice was not a consequence of reduced DSS intake, since water consumption was equivalent between groups during the experiment (data not shown). This data demonstrates clearly that Bcl-3 contributes to colitis.

Macroscopic analysis of colon tissue was performed on day eight after the beginning of DSS treatment. WT DSS-treated mice demonstrated significant shortening of the colon when compared to untreated controls ($p<0.05$; Figure 2C). Surprisingly, a similar degree of colon shortening was observed in DSS treated Bcl-3$^{-/-}$ mice when compared to untreated Bcl-3$^{-/-}$ controls (Figure 2C). Moreover, the significantly increased colonic weight of DSS treated

WT mice relative to untreated controls was also observed in DSS treated Bcl-3$^{-/-}$ mice ($p<0.05$ Figure 2D). Thus, although the macroscopic inflammation of colonic tissue was similar in both DSS treated WT and Bcl-3$^{-/-}$ mice, the clinical indices of the DSS-induced colitis, in particular weight loss, were significantly reduced in Bcl-3$^{-/-}$ mice.

Bcl-3$^{-/-}$ mice show reduced tissue pathology following DSS treatment.

To further investigate the differences in DSS-induced colitis between WT and Bcl-3$^{-/-}$ mice we performed a histological examination of distal colon tissue sections from untreated and DSS treated WT and Bcl-3$^{-/-}$ mice (Figure 3A). No differences were observed between untreated WT and untreated Bcl-3$^{-/-}$ distal colonic tissue samples by H&E staining. Both WT and Bcl-3$^{-/-}$ mice displayed normal epithelial architecture with intact goblet cells and crypts with no discernible inflammatory influx. DSS treatment of WT mice induced a dramatic alteration in the colonic mucosal tissue with extensive oedema, large cellular infiltrates and a severe loss of tissue organisation with destruction of crypts and loss of goblet cells. Although histological analysis revealed similar levels of oedema and cellular infiltrates in Bcl-3$^{-/-}$ mice there was significantly less destruction of the tissue architecture following DSS treatment (Figure 3A). Quantitative histo-pathology analysis of the distal colon tissue from DSS treated Bcl-3$^{-/-}$ mice revealed significantly reduced epithelium damage and loss of tissue architecture compared to WT mice (Figure 3B). However, there was no significant differences in the extent of inflammation (Figure 3C) and the degree of cellular infiltration and oedema (Figure 3D) between DSS-treated WT and Bcl-3$^{-/-}$ mice. This histological analysis provides insight into the reduced weight loss and overall clinical disease score observed in DSS-treated Bcl-3$^{-/-}$ mice relative to WT mice, which would appear to result from an intact or regenerated epithelium rather than reduced leukocyte infiltration.

DSS induces similar levels of cytokines in the colon of Bcl-3$^{-/-}$ and WT mice

Although histological analysis showed similar levels of oedema and leukocyte infiltration in DSS treated WT and Bcl-3$^{-/-}$ mice, it is possible that the inflammation may be qualitatively different between these groups. In order to characterise the inflammation associated with DSS-induced colitis in Bcl-3$^{-/-}$ mice we next measured inflammatory gene expression by in distal colon tissue from untreated and DSS treated WT and Bcl-3$^{-/-}$ mice using qRT-PCR. Surprisingly, although Bcl-3 has previously been described as a negative regulator of Toll-like receptor induced pro-inflammatory gene expression, we found no significant difference in the expression of TNF-α, IL-6, CXCL1 and IL-1β between DSS-treated WT and Bcl-3$^{-/-}$ mice (Figure 4A).

Recent studies have identified a protective role for the cytokines IL-17A and IL-22 [22-24] in DSS colitis by inducing anti-bacterial peptide expression and epithelial cell regeneration in the colon. To assess any role for these cytokines in the observed resistance of Bcl-3$^{-/-}$ mice to DSS induced colitis and maintenance of intestinal epithelium we next measured their expression in the colon of WT and Bcl-3$^{-/-}$ mice. In line with previous reports, the expression of both IL-17A and IL-22 is robustly induced by DSS treatment in WT mice, however no significant differences in the expression of these cytokines was found between DSS treated WT and Bcl-3$^{-/-}$ mice (Figure 4B). We next analysed the cellular composition of the leukocyte infiltrates in DSS-treated WT and Bcl-3$^{-/-}$ mice using immunofluorescence microscopy and antibodies against the cell surface markers F4/80 (macrophage), CD3 (T Cell), Ly6G (neutrophil) and CD11c (dendritic cells) (Figure 5A). Quantitative analysis of tissue sections demonstrated recruitment of macrophage, neutrophils and to a lesser degree T Cells and dendritic cells to the distal colon of DSS treated mice. No significant differences in

the recruitment of these cell types was found between WT and Bcl-3$^{-/-}$ mice (Figure 5B). These data demonstrate that the inflammatory component of DSS-induced colitis is similar between WT and Bcl-3$^{-/-}$ mice and suggest that the reduced susceptibility of Bcl-3$^{-/-}$ mice may result from altered epithelial responses to treatment.

Increased epithelial cell proliferation in DSS treated Bcl-3$^{-/-}$ mice

Since DSS induces epithelial cell damage to initiate colonic inflammation and colitis we next measured cell death in the colon of WT and Bcl-3$^{-/-}$ mice using terminal dUTP nick end labelling (TUNEL) of tissue sections followed by fluorescence microscopy analysis. In both untreated WT and untreated Bcl-3$^{-/-}$ mice we observed a small number of TUNEL positive nuclei in the top of the crypt representing the normal turnover of epithelial cells in this tissue (Figure 6A). However, following DSS treatment we observed a dramatic increase in TUNEL positive cells in both WT and Bcl-3$^{-/-}$ mice. Quantitative analysis of TUNEL staining demonstrated no significant differences in the number of cells undergoing apoptosis in both groups. Immunoblot analysis of caspase-3 cleavage in colonic tissues also demonstrated a significant increase DSS induced apoptosis in WT and Bcl-3$^{-/-}$ mice following DSS treatment (Figure 6B). Densiometric analysis of cleaved caspase-3 levels normalised to β-actin level revealed no significant difference between WT and Bcl-3$^{-/-}$ mice (supplementary Figure 2). Analysis of the mRNA levels of the apoptotic regulators PUMA, Bcl-XL, cIAP1/2 and NOXA by qRT-PCR also revealed no significant differences expression between WT and Bcl-3$^{-/-}$ mice (Figure 6C).

We next assessed epithelial cell proliferation in tissue sections using the cell proliferation marker Ki67. Immunofluorescence microscopy analysis of untreated WT and Bcl-3$^{-/-}$ mucosal colonic tissue revealed equivalent numbers of Ki67 positive cells at the base

of the crypts (Figure 7A and B). Ki67 staining was largely absent in WT mucosal tissue following DSS treatment and coincided with the extensive destruction and loss of tissue architecture (Figure 3). In contrast, widespread and strong Ki67 staining was found throughout the crypts of colonic tissue taken from DSS-treated Bcl-3$^{-/-}$ mice, indicating significantly enhanced proliferation of Bcl-3$^{-/-}$ epithelial cells following treatment (Figure 7A). Immunofluorescence microscopy analysis of Bcl-3 protein in tissue sections was unsuccessful using commercially available antibodies; however previous studies have demonstrated Bcl-3 mRNA expression in intestinal epithelial cells [25-26]. Taken together these data suggest that Bcl-3$^{-/-}$ mice develop less severe clinical and histopathological colitis due to an increase in epithelial proliferation, which leads to regeneration of the damaged epithelium. Our data also demonstrate that this regeneration occurs despite the presence of on-going inflammation in the colonic mucosa.

Discussion

In this study we investigated the expression of Bcl-3 in human IBD and also the role of Bcl-3 in DSS-induced colitis in the mouse. We found that Bcl-3$^{-/-}$ mice develop less severe colitis compared to littermate control wild type mice. These findings were unexpected given the previously described role of Bcl-3 as a negative regulator of inflammatory gene expression[16] and the recent identification of reduced Bcl-3 expression as potential risk factors for Crohn's disease[17]. However, the resistance of Bcl-3$^{-/-}$ mice to experimentally induced colitis correlates with our analysis of Bcl-3 expression in the colon of IBD patients which was significantly increased when compared to healthy individuals. It is possible that the identified SNPs may lead to increased Bcl-3 expression rather than decreased expression as predicted. Thus, our findings suggest that increased expression of Bcl-3 rather than reduced expression may be a potential risk factor for IBD. Our study also identifies a novel role for Bcl-3 in regulating intestinal epithelial cell proliferation during DSS-induced colitis.

Analysis of cytokine expression during DSS-induced colitis in Bcl-3$^{-/-}$ mice revealed a robust inflammatory response following DSS treatment characterised by significantly elevated levels of pro-inflammatory cytokines TNFα, IL-6 and IL-1β. The levels of these cytokines was similar to WT mice indicating that Bcl-3 does not act as a negative regulator of TNFα, IL-6 and IL-1β expression in the context of DSS-induced colonic inflammation. Histological analysis further supported this observation as significant oedema and leukocyte infiltration were present in Bcl-3$^{-/-}$ colonic tissue sections and to a similar degree as that seen in WT mice. Furthermore, equivalent composition of cellular infiltrates was observed between WT and Bcl-3$^{-/-}$ mice which demonstrated that the inflammation was qualitatively, as well as quantitatively, similar to WT mice. This data suggests that Bcl-3 may not play a significant role in the regulation of inflammation in the colon.

Despite a robust inflammatory response following DSS treatment, the colonic tissue architecture in Bcl-3$^{-/-}$ mice, in particular the epithelial features remain intact. Following DSS treatment intestinal epithelial cell proliferation in Bcl-3$^{-/-}$ mice was significantly enhanced whereas in WT mice it was absent. The increased proliferation in Bcl-3$^{-/-}$ mice correlates with the maintenance of tissue architecture and structure and suggests that the resistance to DSS-induced colitis of Bcl-3$^{-/-}$ mice results from increased regeneration of the epithelium. It is also noteworthy that Bcl-3 acts a negative regulator of myeloid progenitor proliferation and differentiation, and is essential for limiting granulopoiesis under inflammatory conditions[26]. This study identifies a novel role for Bcl-3 in regulating intestinal epithelial cell proliferation under inflammatory but not homeostatic conditions. Our identification of Bcl-3 as a negative regulator of intestinal epithelial cell proliferation during colitis suggests additional physiological functions for Bcl-3 beyond its role as a negative regulator of pro-inflammatory gene expression.

The dual role of NF-κB as a key mediator of inflammation and a critical driver of epithelial cell survival and proliferation has rendered it a complex and difficult therapeutic target in IBD. Transgenic mice in which NF-κB activity has been selectively inhibited in the intestinal epithelium develop spontaneous colitis due to failure of the epithelial barrier function while an increase in intestinal NF-κB activity also leads to severe inflammation[4]. The data obtained in this study however suggests that certain regulatory components of the NF-κB pathway such as Bcl-3 may play a more important role in the epithelium rather than the immune system in the colon. We have previously demonstrated that Bcl-3 expression is induced by inflammation[16]. Given that the proliferation of intestinal epithelial cells is normal in Bcl-3$^{-/-}$ mice it is likely that inflammation induced expression of Bcl-3 in the epithelium during colitis contributes to the development of disease. Thus, by targeting Bcl-3 it may be possible to enhance epithelial cell proliferation and regeneration without

exacerbating inflammation in the intestine. The potential therapeutic benefits to IBD are highlighted by the reduced clinical score and lack of weight loss in DSS-treated Bcl-3$^{-/-}$ mice.

In summary, we describe a novel function for Bcl-3 in regulating epithelial cell proliferation during DSS-induced colitis. The increased epithelial cell proliferation and regeneration in Bcl-3$^{-/-}$ mice further supports a role for NF-κB in maintaining the integrity of the intestinal epithelium. This report suggests that targeting Bcl-3 in colitis may be therapeutically beneficial in IBD through increasing tissue regeneration and repair in the colon without exacerbating the inflammatory response.

Acknowledgements

This research was supported by Science Foundation Ireland (Grant 08/IN.1/B1843 and CSET grant 07/CE/B1368) and the Marie Curie International Re-integration Grant programme.

Figure Legends

Figure 1

BCL-3 expression in IBD. (**A**) Bcl-3 mRNA levels in Crohn's disease (CD, n=11) and ulcerative colitis (UC, n=11) tissue samples relative to normal (N, n=6) controls ($p<0.05$ *) (**B**) Bcl-3 mRNA levels in colon tissue of untreated and DSS treated WT mice. Mice were treated with 2% DSS for 6 days followed by 2 days on normal drinking water before tissue was harvested. Data is expressed as means ± SEM. Statistical significance was determined using Mann Whitney *t* tests.

Figure 2

BCL3$^{-/-}$ mice develop milder DSS induced colitis. (**A**) Weight loss (% change) was measured over time with differences between WT 2% DSS and WT Healthy control found to be statistically significant from day 6 to day 8 ($p<0.01$ ** , $p<0.001$ *** & $p<0.001$ ***) respectively. Differences in weight loss between WT 2% DSS and Bcl-3$^{-/-}$ Healthy control were found to be significant at day 8 ($p<0.001$ ***). (**B**) Differences in Disease activity index (DAI) scores were observed starting from day 5 to day 8 in both WT and Bcl-3$^{-/-}$ DSS groups relative to both Healthy controls ($p<0.001$ ***). Differences in weight loss and DAI score were calculated over time by Two-way ANOVA with Bonferroni post hoc test. (**C-D**) Differences in colon length and distal colon weight between in both WT and Bcl-3$^{-/-}$ mice was relative to Healthy controls were found to be statistically significant ($p<0.05$) Data is expressed as mean ± SEM. Statistical significance was determined using Mann Whitney *t* Tests (n=7/group).

Figure 3

Reduced histological damage in Bcl-3$^{-/-}$ mice following DSS induced colitis. (**A**) Representative H&E of untreated (control) and DSS treated wild type (WT) and Bcl-3$^{-/-}$ mice. Histological sections were scored for cellular infiltration (**B**), extent of injury (**C**), and epithelium, and crypt damage (**D**). DSS induced cellular infiltration, extent of injury, and epithelium and crypt damage scores were increased in WT and Bcl-3$^{-/-}$ mice relative to untreated controls ($p<0.05$). DSS treated WT mice showed greater crypt and epithelium damage relative to DSS treated and Bcl-3$^{-/-}$ mice ($p<0.01$). Data is representative of greater than 7 fields of view per tissue section at 20X (n=7 per group).

Figure 4

Normal inflammatory cytokine expression in mucosal tissue of DSS-treated Bcl-3$^{-/-}$ mice. Distal colon tissues were analysed for changes immune gene expression relative to the housekeeping gene 18s rRNA. (**A**) Increased pro-inflammatory gene expression was found in the DSS group of WT and Bcl-3$^{-/-}$ mice relative to untreated control groups ($p<0.05$*). No statistical significance in gene expression changes was observed between WT and Bcl-3$^{-/-}$ mice (**B**) Increased IL-17A and IL-22 gene expression in DSS treated WT and Bcl-3$^{-/-}$ mice relative to untreated controls. Data is represented as relative mRNA expression as determined by the 2-ΔΔCT method. Statistical significance was calculated using Mann Whitney *t* tests ($p<0.05$ *). Data expressed as mean ± SEM (n= 7).

Figure 5

Analysis of inflammatory infiltration during colitis in Bcl-3$^{-/-}$ mice (**A**) Immunofluorescent staining of 6μm distal colon section at 40X for macrophages (F/480), Dentritic cells (CD11c), T cells (CD3) and neutrophils (Ly6G). (**B**) Quantification of F4/80, CD3, Ly6G and CD11c positive cellular populations was performed on 7 fields of view per section. Data is representative of scoring of all sections per treatment group. N=7.

Figure 6

Analysis of cell death during colitis in Bcl-3$^{-/-}$ mice (**A**) TUNEL stained distal colon 6μm section. Arrows indicate TUNEL positive cells. Quantification of TUNEL positive cells were was performed on 7 fields of view per tissue section at 20X (n=7 per group). (**B**) Western blotting for inactive (32KDa) and active (17KDa) caspase-3 in distal colon tissue of control and DSS treated WT and Bcl-3$^{-/-}$ mice. (**C**) QPCR analysis of PUMA, Bcl-XL, cIAP1/2 and NOXA mRNA in distal colon tissue of control and DSS treated WT and Bcl-3$^{-/-}$ mice.

Figure 7

Elevated cellular proliferation in DSS treated Bcl-3$^{-/-}$ mice. (**A**) Ki67 immunofluorescence staining of 6μm distal colon sections. Data is representative of greater than 7 fields of View per tissue section at 20X (n=7 per group). Inset, magnified section of Ki76 positive cells indicated by arrow head. (**B**) Quantification of Ki67 positive cells was performed on 7 fields of view per tissue section at 20X (n=7 per group).

References

1. Ghosh S, Hayden MS. New regulators of NF-[kappa]B in inflammation. Nat Rev Immunol 2008; 8:837-48.
2. Hayden MS, Ghosh S. Shared Principles in NF-κB Signaling. Cell 2008; 132:344-62.
3. Schreiber S, Nikolaus S, Hampe J. Activation of nuclear factor κB in inflammatory bowel disease. Gut 1998; 42:477-84.
4. Wullaert A, Bonnet MC, Pasparakis M. NF-[kappa]B in the regulation of epithelial homeostasis and inflammation. Cell Res 2011; 21:146-58.
5. Karrasch T, Kim J-S, Muhlbauer M, Magness ST, Jobin C. Gnotobiotic IL-10−/−;NF-κBEGFP Mice Reveal the Critical Role of TLR/NF-κB Signaling in Commensal Bacteria-Induced Colitis. The Journal of Immunology 2007; 178:6522-32.
6. Vereecke L, Sze M, Guire CM, Rogiers B, Chu Y, Schmidt-Supprian M, Pasparakis M, Beyaert R, van Loo G. Enterocyte-specific A20 deficiency sensitizes to tumor necrosis factor–induced toxicity and experimental colitis. The Journal of Experimental Medicine 2010; 207:1513-23.
7. Zhang J, Stirling B, Temmerman ST, Ma CA, Fuss IJ, Derry JMJ, Jain A. Impaired regulation of NF-κB and increased susceptibility to colitis-associated tumorigenesis in CYLD-deficient mice. The Journal of Clinical Investigation 2006; 116:3042-9.
8. Neurath MF, Pettersson S, Meyer Zum Buschenfelde K-H, Strober W. Local administration of antisense phosphorothiate olignucleotides to the p65 subunit of NF-[kappa]B abrogates established experimental colitis in mice. Nat Med 1996; 2:998-1004.
9. Nenci A, Becker C, Wullaert A, Gareus R, van Loo G, Danese S, Huth M, Nikolaev A, Neufert C, Madison B, Gumucio D, Neurath MF, Pasparakis M. Epithelial NEMO links innate immunity to chronic intestinal inflammation. Nature 2007; 446:557-61.
10. Steinbrecher KA, Harmel-Laws E, Sitcheran R, Baldwin AS. Loss of Epithelial RelA Results in Deregulated Intestinal Proliferative/Apoptotic Homeostasis and Susceptibility to Inflammation. The Journal of Immunology 2008; 180:2588-99.
11. Araki A, Kanai T, Ishikura T, Makita S, Uraushihara K, Iiyama R, Totsuka T, Takeda K, Akira S, Watanabe M. MyD88-deficient mice develop severe intestinal inflammation in dextran sodium sulfate colitis. Journal of Gastroenterology 2005; 40:16-23.
12. Rakoff-Nahoum S, Paglino J, Eslami-Varzaneh F, Edberg S, Medzhitov R. Recognition of Commensal Microflora by Toll-Like Receptors Is Required for Intestinal Homeostasis. Cell 2004; 118:229-41.
13. Kerr LD, Duckett CS, Wamsley P, Zhang Q, Chiao P, Nabel G, McKeithan TW, Baeuerle PA, Verma IM. The proto-oncogene bcl-3 encodes an I kappa B protein. Genes & Development 1992; 6:2352-63.
14. Nolan GP, Fujita T, Bhatia K, Huppi C, Liou HC, Scott ML, Baltimore D. The bcl-3 proto-oncogene encodes a nuclear I kappa B-like molecule that preferentially interacts with NF-kappa B p50 and p52 in a phosphorylation-dependent manner. Molecular and Cellular Biology 1993; 13:3557-66.
15. Schwarz EM, Krimpenfort P, Berns A, Verma IM. Immunological defects in mice with a targeted disruption in Bcl-3. Genes & Development 1997; 11:187-97.

16. Carmody RJ, Ruan Q, Palmer S, Hilliard B, Chen YH. Negative Regulation of Toll-Like Receptor Signaling by NF-κB p50 Ubiquitination Blockade. Science 2007; 317:675-8.
17. Fransen K, Visschedijk MC, van Sommeren S, Fu JY, Franke L, Festen EAM, Stokkers PCF, van Bodegraven AA, Crusius JBA, Hommes DW, Zanen P, de Jong DJ, Wijmenga C, van Diemen CC, Weersma RK. Analysis of SNPs with an effect on gene expression identifies UBE2L3 and BCL3 as potential new risk genes for Crohn's disease. Human Molecular Genetics 2010; 19:3482-8.
18. Murphy CT, Moloney G, MacSharry J, Haynes A, Faivre E, Quinlan A, McLean PG, Lee K, O'Mahony L, Shanahan F, Melgar S, Nally K. Technical Advance: Function and efficacy of an α4-integrin antagonist using bioluminescence imaging to detect leukocyte trafficking in murine experimental colitis. Journal of Leukocyte Biology 2010; 88:1271-8.
19. Cummins EP, Seeballuck F, Keely SJ, Mangan NE, Callanan JJ, Fallon PG, Taylor CT. The Hydroxylase Inhibitor Dimethyloxalylglycine Is Protective in a Murine Model of Colitis. Gastroenterology 2008; 134:156-65.e1.
20. Tambuwala MM, Cummins EP, Lenihan CR, Kiss J, Stauch M, Scholz CC, Fraisl P, Lasitschka F, Mollenhauer M, Saunders SP, Maxwell PH, Carmeliet P, Fallon PG, Schneider M, Taylor CT. Loss of Prolyl Hydroxylase-1 Protects Against Colitis Through Reduced Epithelial Cell Apoptosis and Increased Barrier Function. Gastroenterology 2010; 139:2093-101.
21. Costello CM, Mah N, Häsler R, Rosenstiel P, Waetzig GH, Hahn A, Lu T, Gurbuz Y, Nikolaus S, Albrecht M, Hampe J, Lucius R, Klöppel G, Eickhoff H, Lehrach H, Lengauer T, Schreiber S. Dissection of the Inflammatory Bowel Disease Transcriptome Using Genome-Wide cDNA Microarrays. PLoS Med 2005; 2:e199.
22. Zenewicz LA, Yancopoulos GD, Valenzuela DM, Murphy AJ, Stevens S, Flavell RA. Innate and Adaptive Interleukin-22 Protects Mice from Inflammatory Bowel Disease. Immunity 2008; 29:947-57.
23. Ota N, Wong K, Valdez PA, Zheng Y, Crellin NK, Diehl L, Ouyang W. IL-22 bridges the lymphotoxin pathway with the maintenance of colonic lymphoid structures during infection with Citrobacter rodentium. Nat Immunol 2011; 12:941-8.
24. O'Connor Jr W, Kamanaka M, Booth CJ, Town T, Nakae S, Iwakura Y, Kolls JK, Flavell RA. A protective function for interleukin 17A in T cell-mediated intestinal inflammation. Nat Immunol 2009; 10:603-9.
25. Dann SM, Spehlmann ME, Hammond DC, Iimura M, Hase K, Choi LJ, Hanson E, Eckmann L. IL-6-Dependent Mucosal Protection Prevents Establishment of a Microbial Niche for Attaching/Effacing Lesion-Forming Enteric Bacterial Pathogens. The Journal of Immunology 2008; 180:6816-26.
26. Tao Y, Drabik KA, Waypa TS, Musch MW, Alverdy JC, Schneewind O, Chang EB, Petrof EO. Soluble factors from Lactobacillus GG activate MAPKs and induce cytoprotective heat shock proteins in intestinal epithelial cells. American Journal of Physiology - Cell Physiology 2006; 290:C1018-C30.
27. Kreisel D, Sugimoto S, Tietjens J, Zhu J, Yamamoto S, Krupnick AS, Carmody RJ, Gelman AE. Bcl3 prevents acute inflammatory lung injury in mice by restraining emergency granulopoiesis. The Journal of Clinical Investigation 2011; 121:265-76.

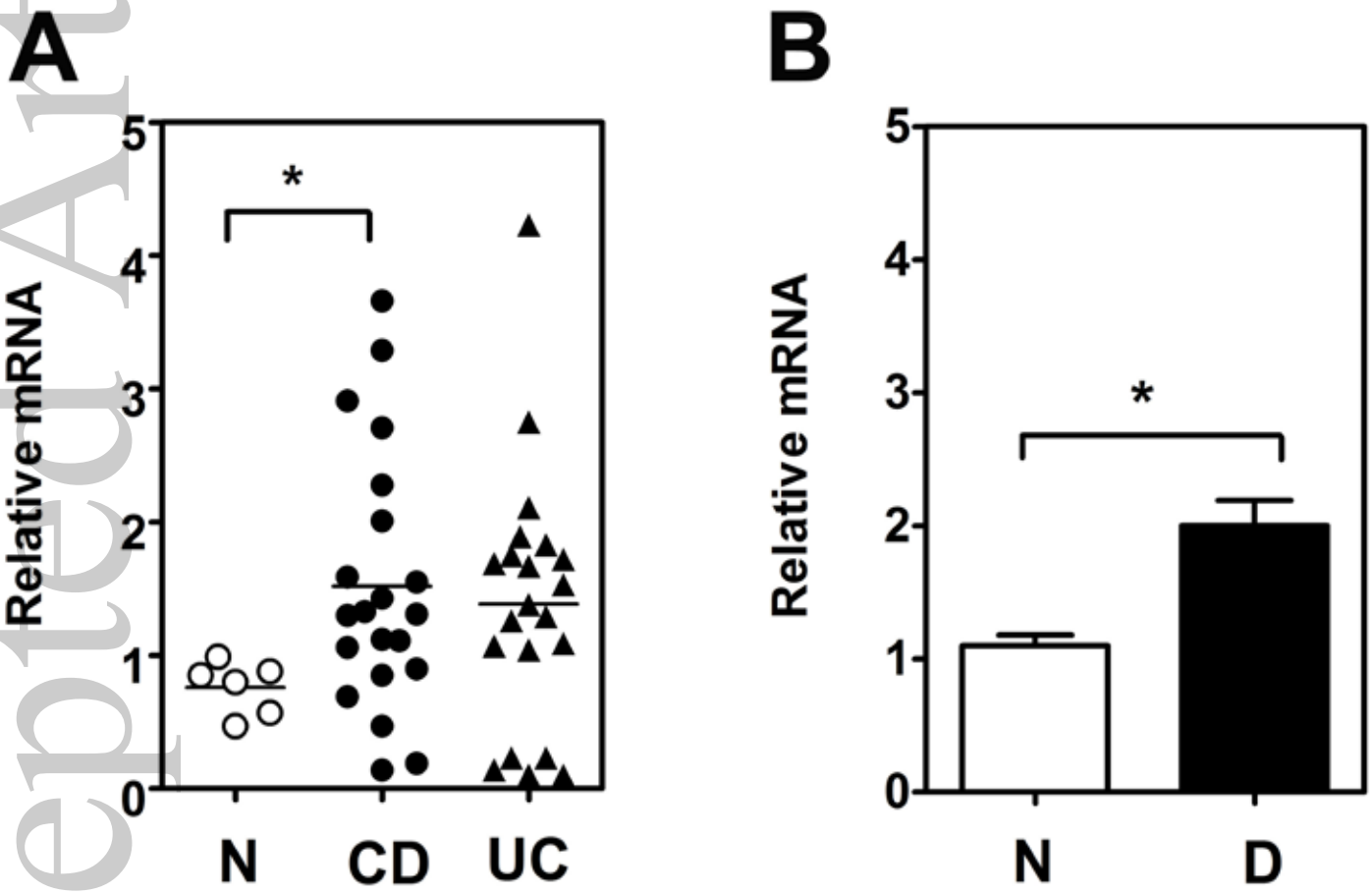

figure 1.tif

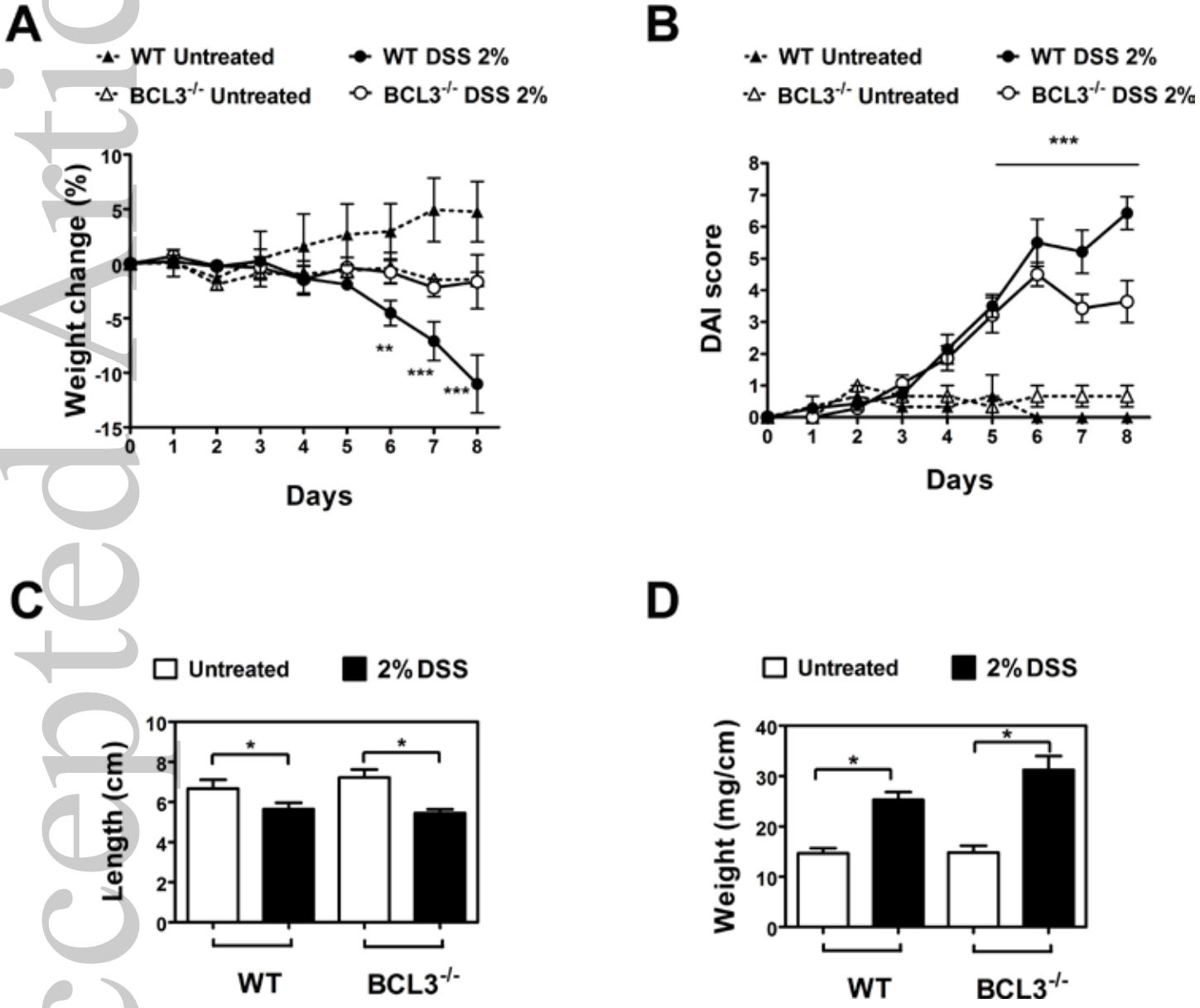

figure 2.jpg

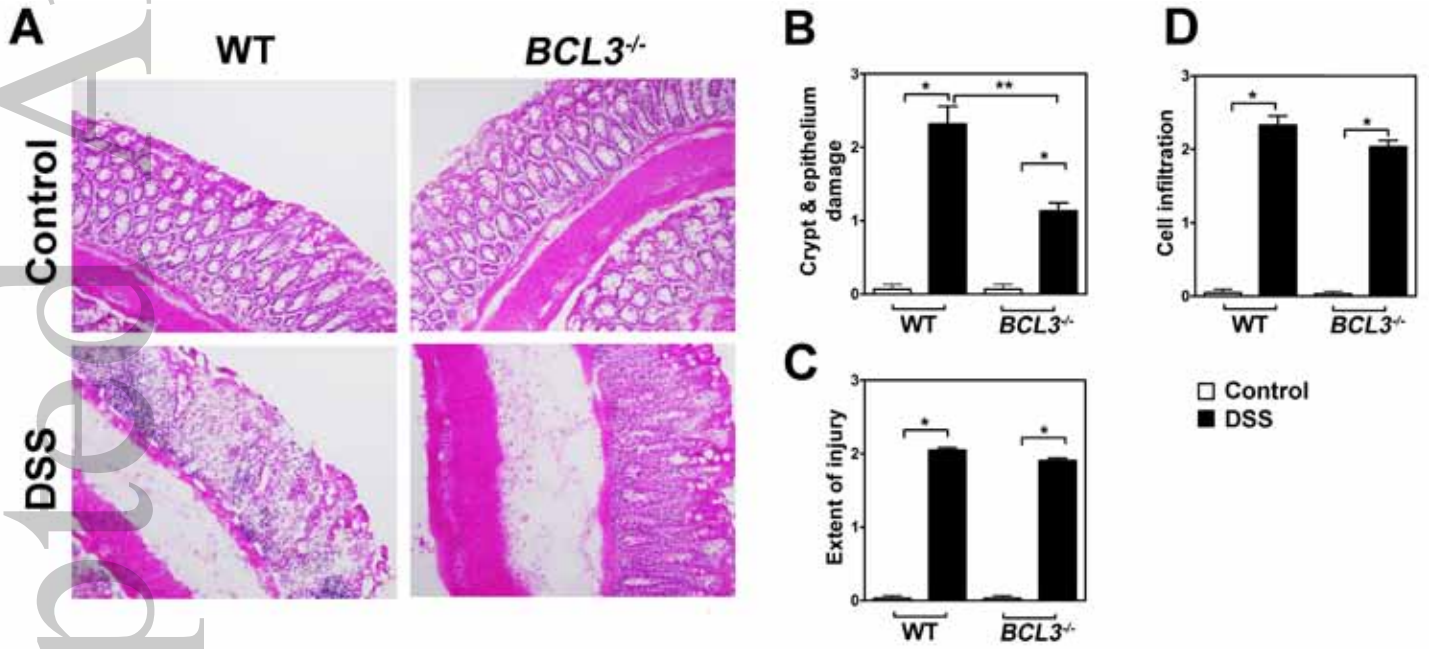

figure 3.jpg

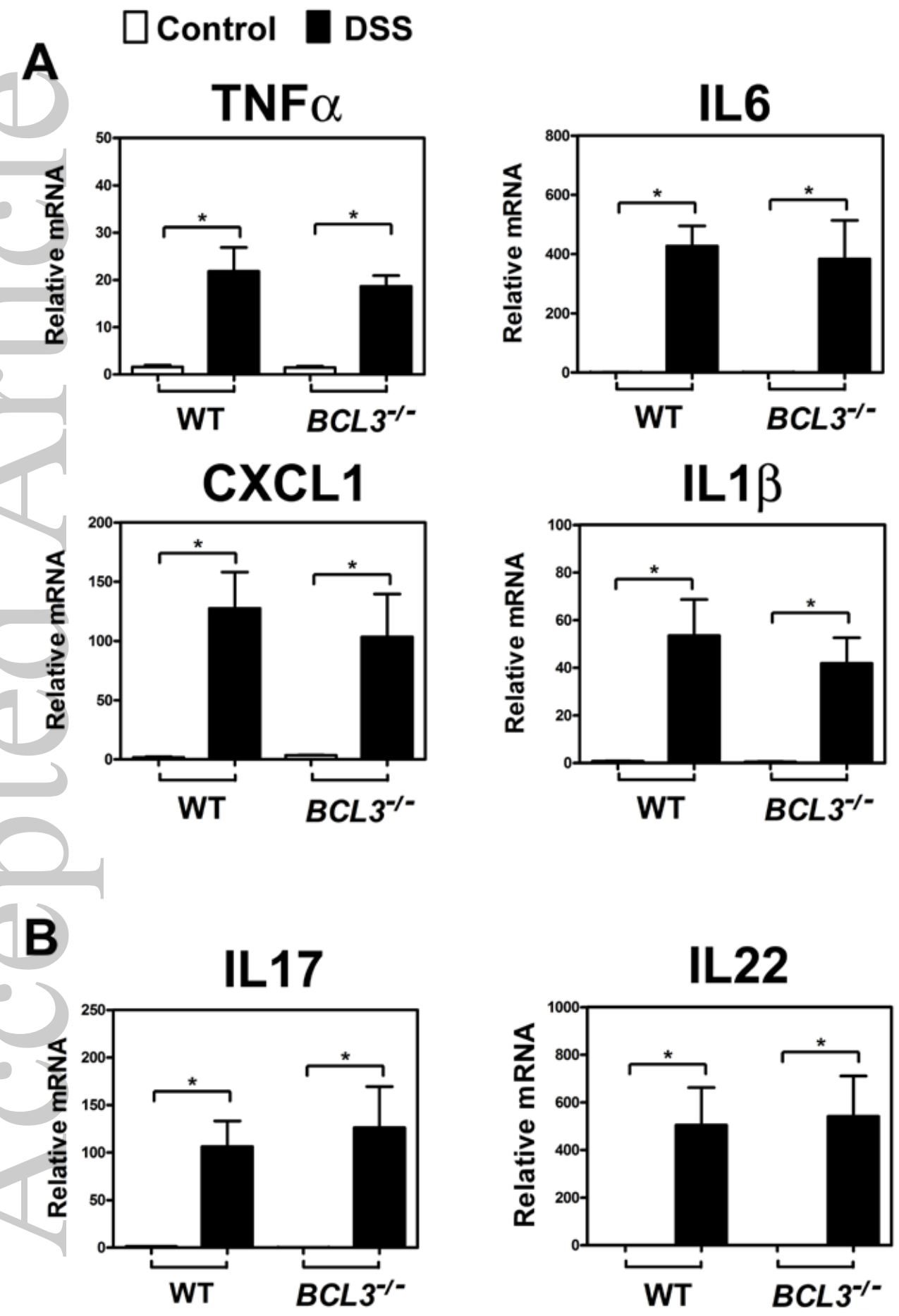

figure 4..jpg

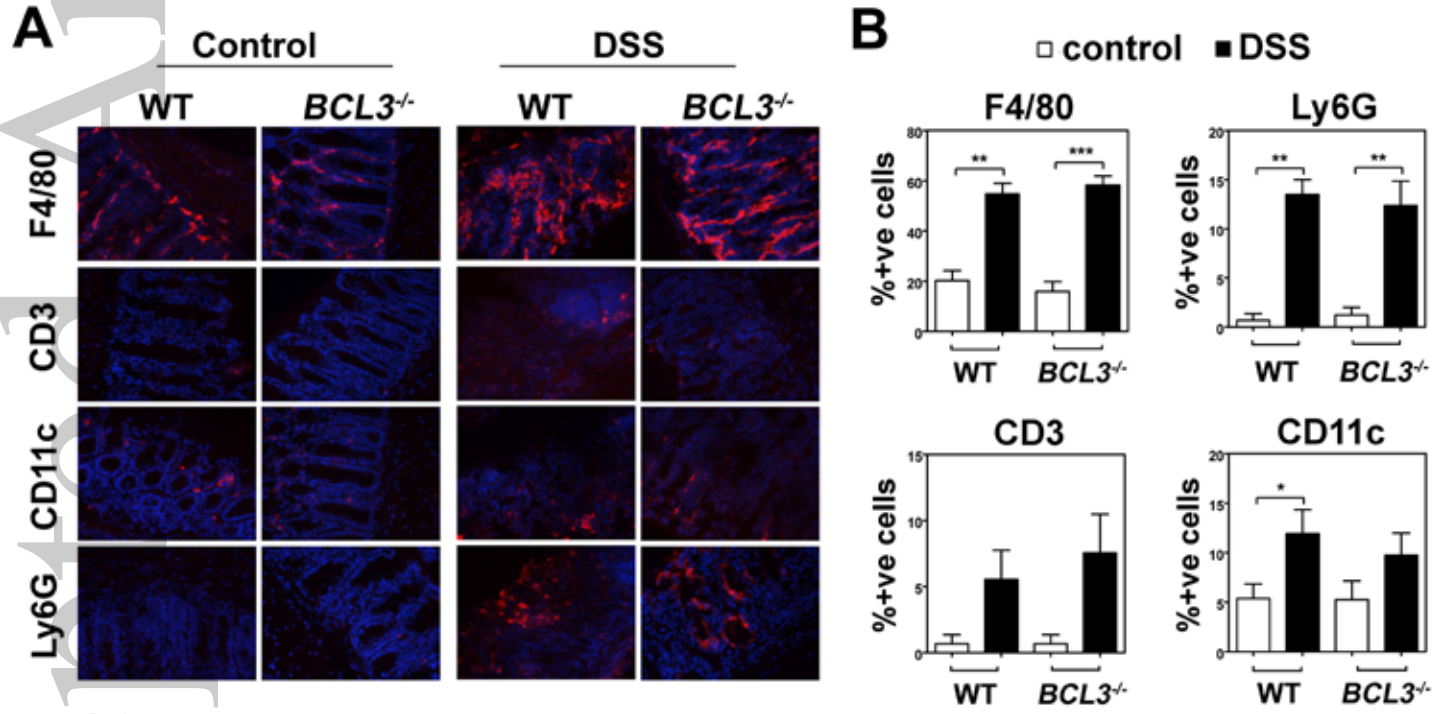

figure 5.jpg

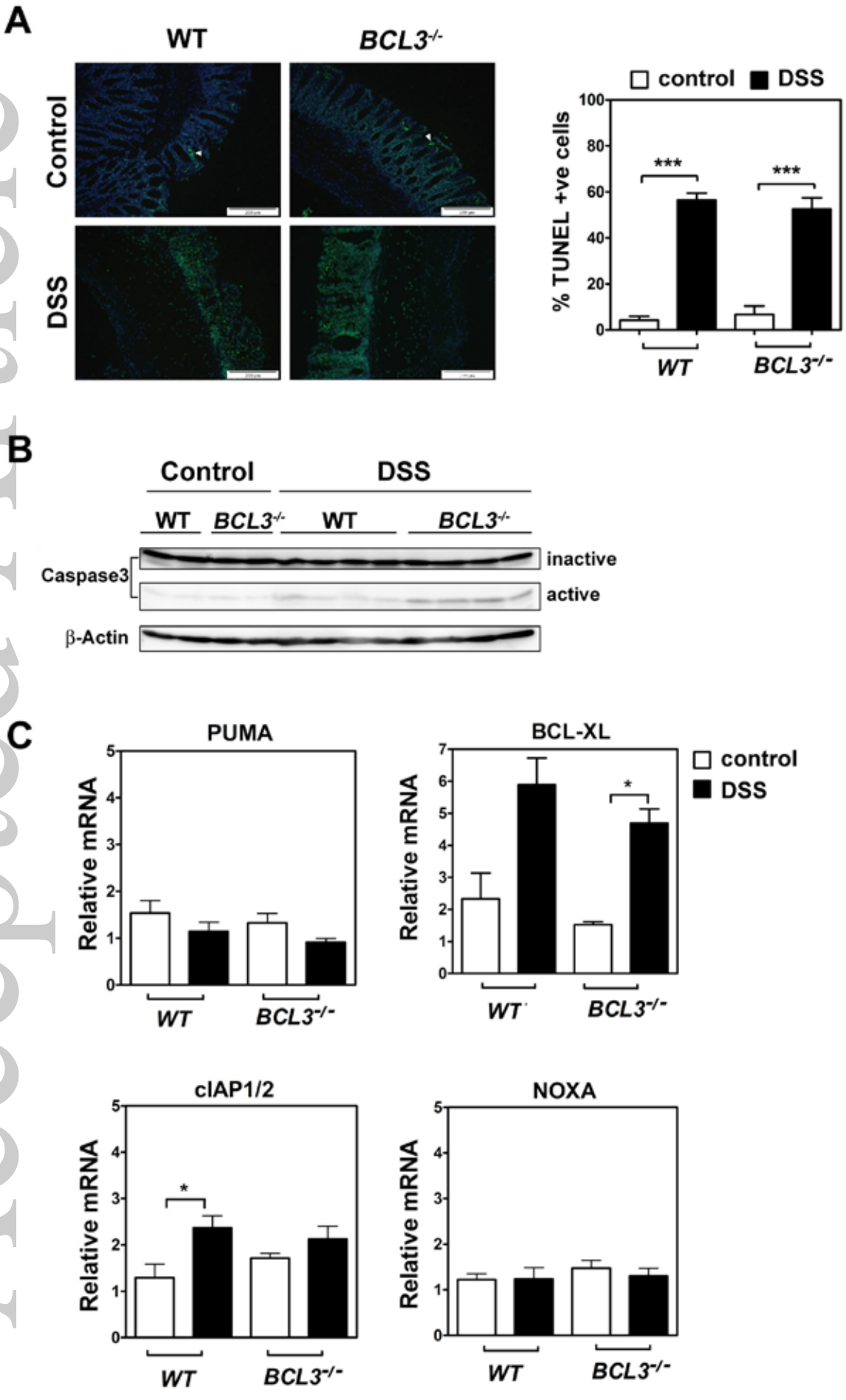

figure 6.jpg

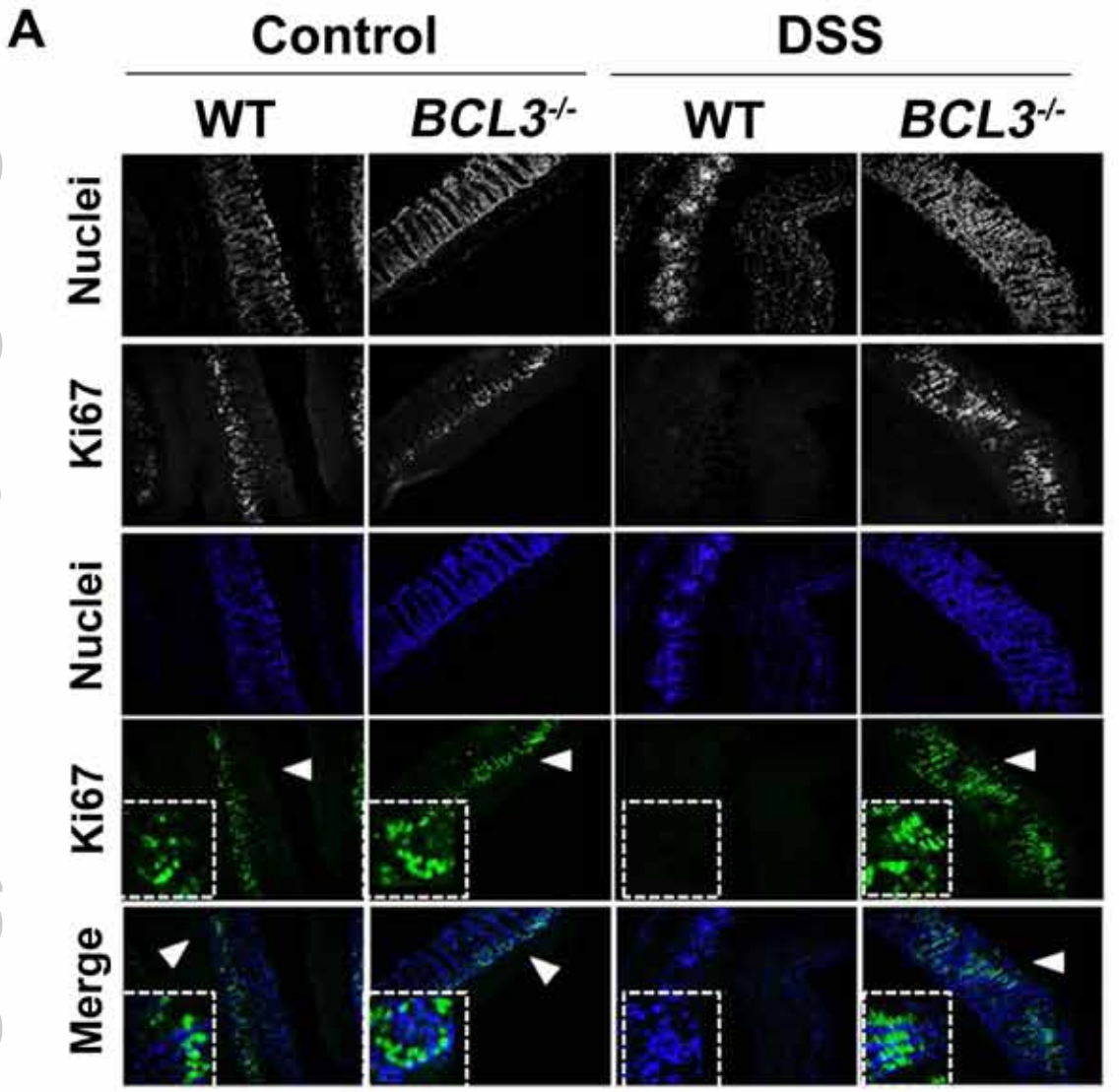

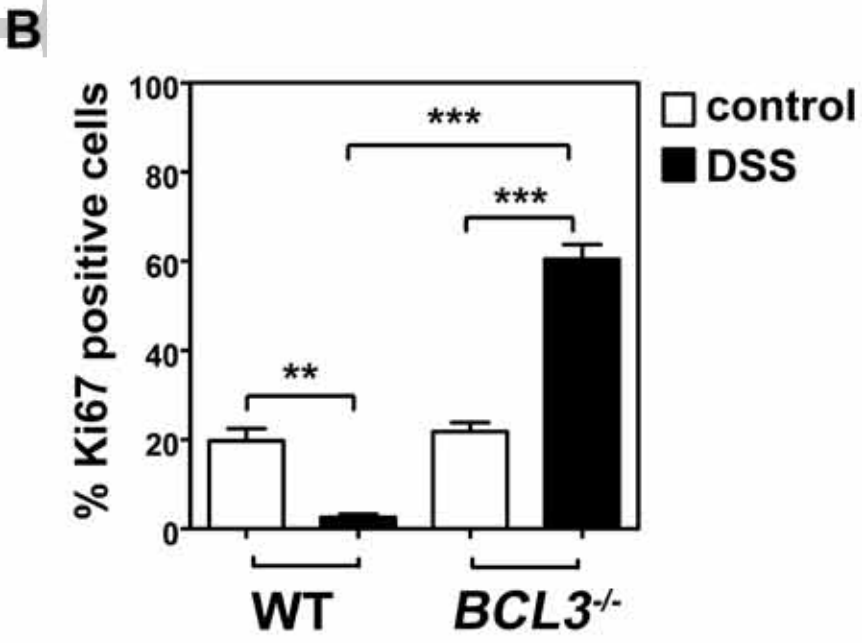

figure 7.jpg